Desalination and Water Treatment
www.deswater.com

36 (2011) 105–118
December

1944-3994/1944-3986
doi: 10.5004/dwt.2011.2177

Prediction of metal ion rejection in electro-cross-flow ultrafiltration using an artificial neural network

Ana Ames[a], Eduardo Rogel-Hernandez[a], Shui Wai Lin[b], Lucía Z. Flores-López[b], Juan Ramón Castro[a], Fernando T. Wakida[a], Samuel Melendez[a], Heriberto Espinoza-Gomez[a,*]

[a]*Facultad de Ciencias Químicas e Ingeniería, Universidad Autónoma de Baja California, Calzada Universidad 14418, Parque Industrial Internacional, C.P. 22390, Tijuana, B.C., México.*
Tel.: +526649797500; Fax: +526646822790; e-mail: hespinoza@uabc.edu.mx
[b]*Centro de Graduados e Investigación, Instituto Tecnológico de Tijuana, A.P. 1166, C.P. 22000, Tijuana, B.C., Mexico*

Received 28 June 2010; accepted 1 May 2011

ABSTRACT

We studied an electro-cross flow ultrafiltration system that uses charged and neutral ultrafiltration membranes and changes in pH and voltage to Pb^{2+}, Ca^{2+} and Fe^{2+}. Simulation of the experimental data was performed with the aid of an artificial neural network (ANN), to obtain a mathematical model to predict metal ion remotion. Analysis of the experimental data indicates that the surface charge of the membrane does not affect the removal process. However, the neutral membrane (SP1) has a higher flux (0.293 L/m^2 s) than the charged membrane (AC1) (0.271 L/m^2 s). Our results also indicate that the metal ions studied are efficiently removed by applying voltage. In all cases, by applying a voltage of 1.0 V for 30 min to an AC1 membrane, metal ion removal was well over 90%. The ANN model developed properly adjusted the experimental data with a non-linear model and allowed us to predict with a standard deviation no greater than 10% the removal rate as a function of voltage and time. In addition, a simplified model prediction suggests that the removal percentage is dependent only with time at a fixed voltage. This model allowed us also to observe the speed with which the system stabilizes to achieve the maximum removal percentage.

Keywords: Electro-cross flow; Neural Networks; Heavy metal ions; Ultrafiltration

1. Introduction

One of the main environmental concerns today is the removal of metals from polluted wastewater, because of their high toxicity to humans and many other forms of life. One of the main sources of metals in wastewater comes from chemical industries, especially from those whose processes involve metal plating. The removal of metals from wastewater by membrane technology is a valid alternative form of separation that has proven effective, its main drawback is a process called ''membrane fouling'' which leads to a decrease in the permeate flow rate or the useful lifetime of the membrane.

Nanofiltration (NF) membranes are a relatively new class of membranes that have properties between ultrafiltration (UF) and reverse osmosis (RO) membranes [1].

*Corresponding author

Some of the main applications of NF membranes have focused on the removal of salts in water treatment. Several authors report that the operation of a NF membrane depends on the combination of two principles, which lead to ion exclusion: membrane pore size and dielectric properties [1–3]. In the case of dielectric exclusion, a difference in electric potential must exist in the interphase between the membrane and the solution, this electric potential is also known as the Donnan effect. The Donnan effect predicts the movements of ions counter to cross-flow from the solution and the movement ions in the direction of flow in parallel with the phase of the membrane.

When the diameters of the membrane pores are bigger, than the electrolyte ions, as in the UF membranes, the electrostatic effect is mainly responsible for electrolyte permeation [4]. In this study, we used an UF system coupled to an electrode system, seeking to increase the effect of the electrostatic force on the removal of divalent ions present in the wastewater samples, and test whether an increased electrical charge increases the efficiency/effectiveness of UF membranes with a pore size greater than that of the ions. In order to incorporate additional electrostatic forces to the surface charge of the membrane (Donnan effect), our group developed an electro-cross-flow module, selecting UF membranes. [5]. The mechanism of the electro-cross-flow UF system used suggests that repulsion and/or rejection of ions is based on their charge (valence) and the charge density applied to the electrodes. Unlike electrodialysis, where the ions pass through an ion-selective membrane, in our electro-cross-flow UF system the ions are rejected and concentrated in the water leaving the system, mainly due to the charge density on the electrodes.

Several theoretical models describe the behavior of mass transfer across the membrane [6–9]. These models are based on diffusion, adsorption, and concentration-polarization, among others. The key points of these models are based on structural parameters and/or electrical properties of the membrane.

Solute transport across the membrane can be described by irreversible thermodynamics, in which the membrane is treated as a ''black box''. In the pressure drop for membrane processes such as RO, NF and UF, the final solute flux can be described as the addition of convective and diffusive fluxes [10]. Previously reported models used to predict the behavior of UF membranes, are not adequate for the system under study, since working with solutes in the ionic form, we should not consider the part of the model that attributes ion removal only to size exclusion. Other reported models for RO and NF membranes include the Donnan effect in addition to pore size exclusion.

Since, the ion removal mechanism that promotes the effective rejection of ions in our electro-cross-flow UF system is still unknown. We have considered using a modeling technique that would allow us to include several process variables in order to establish a function that describes it. Therefore, an artificial neural network (ANN) was used, since they have a higher predictive capability and are well suited for the approximation of almost any non-linear function [11,12]. In addition, because of their low background it was found that ANNs are a good alternative to the conventional models of black box. ANNs have been applied successfully to different types of membranes: microfiltration [13–16], UF [15], NF [17], dialysis process [18], and ceramic membrane for treatment of oily wastewater [19], also in the prediction of membrane properties before fabrication [20] and the prediction of fouling membrane [21]. Sadrzadeh et al. [22], used ANN to predict separation percent (SP) of lead ions fromwastewater using electrodialysis (ED). The aim was to predict SP of Pb^{2+} as a function of concentration, temperature, flow rate, and voltage. In another study, Bowen et. al. [15,23] applied ANNs for the analysis of cross-flow-filtration using an UF membrane with a single hidden layer of proteins and colloids. They found that the careful selection of the input variables and training points helps in the optimization of the ANN training process and that it can achieve very accurate predictions of the experimental results [1].

In the ANN model we have developed, the voltage and time are handled as input variables and the removal percentage as an output variable, holding constant the membrane structural parameters and functional parameters such as pH, type of divalent ion and salt concentration in the solution, as well as temperature and transmembrane pressure.

This work presents experimental electro-cross-flow filtration data obtained by using two different UF membranes (SP1 and AC1) and three different salts ($PbSO_4$, $FeSO_4$ and $CaSO_4$) at a low concentration in order for them to be fully ionized. The removal of ions is measured at different times until the system reached a steady state. In each experiment conditions such as voltage (0–1.5 V), pH (4, 7 and 11), type of membrane (neutral surface or with negative charge) and salt (type of ion) were fixed. All filtrations were performed at a constant temperature of 25°C and pressure of 4.8 bars.

The main objective of this work was to develop an ANN model which would predict the removal kinetics of each of the three divalent cations studied (Pb^{2+}, Fe^{2+} and Ca^{2+}), that would also allow the study of the effect of voltage on the system.

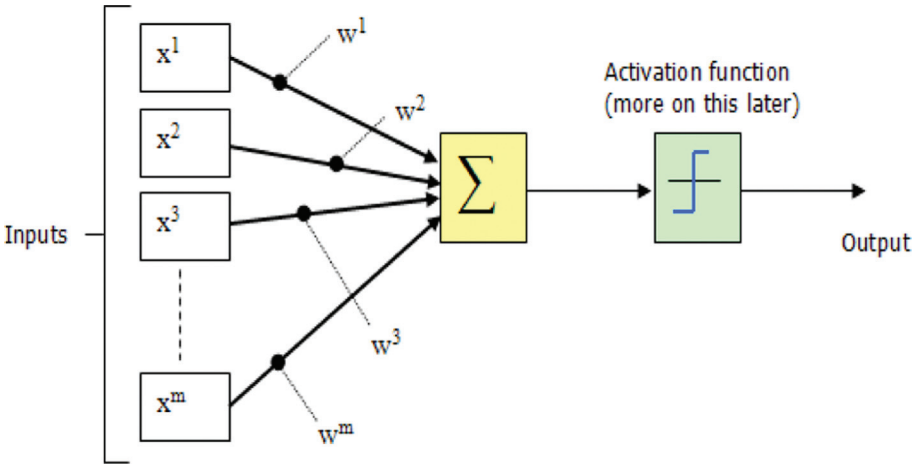

Fig. 1. The architecture of an Artificial Neural Network (ANN).

2. ANNs

An ANN is a parallel-distributed information-processing system with a large number of neurons and connections. The uniqueness of an ANN lies in its ability to learn and generate interrelationships between the input and output of observed (or experimental) data without requiring any postulates or assumptions [24].

Neural models are determined by the topology (structural design of connections and nodes) of the network, the features of the nodes, and the rules or algorithms used for training or learning. The training of a system using its operational data, can allow us to determine the set of weights or synaptic connections of the network, giving it the ability to represent the system under study. The network then becomes an empirical model of the system, which allows the prediction of its output variables, or in the case of a dynamic system, the inference of its behavior over time [25]. A basic neural network comprising three layers: the input, the hidden, and the output layers are shown in Fig. 1. Each node in the input layer of the network brings in the value of one independent variable (x^m). The nodes in the input layer do not perform any processing on the input, thus serving only as a fan-out. The hidden nodes calculate synaptic connection, which is the weighted sum of the inputs by function activation to obtain the output signal. The output layer produces the calculated values of the dependent variable [26].

The mathematical relationship between inputs, hidden layers, and outputs is described by weights (w^m), bias weights, and transfer functions:

The transfer functions used in this study were:

$$f_1 = \log sig = \frac{1}{(1+e^{-x})} \quad (1)$$

$$f_2 = \tan sig = \frac{(e^{x}-e^{-x})}{(e^{x}+e^{-x})} \quad (2)$$

$$f_3 = purelin = x \quad (3)$$

The term training of an ANN refers to the procedures for identifying the numerical values of the parameters in these equations that give the best fit to experimental data [26].

Back propagation is a commonly used training process that propagates the error information backward from the output nodes to the hidden nodes. The error is calculated by comparing the output from the outer layer and the actual target value obtained from the training data. The steepest decent method is also commonly used to find the values of connection weights. Once the network is trained, it could be used as a model for the system [25].

In order for an ANN to perform an acceptable prediction, a set of weights that minimizes the error between target and predicted outputs should be found. The process of finding these weights is called ANN training. During the training process, ANN weights are updated in a systematic way by means of minimizing an error function using any of the known optimization techniques. The error function is usually the sum-square-error between the target and ANN outputs. In order to train a network properly, available data should be divided into two sets, training, and testing. The training set is used for updating weights, and the testing set is used to ensure maximum generalizability. As a result, both the training set will numerically update the weights and the testing set will heuristically pick up the best set of weights [24].

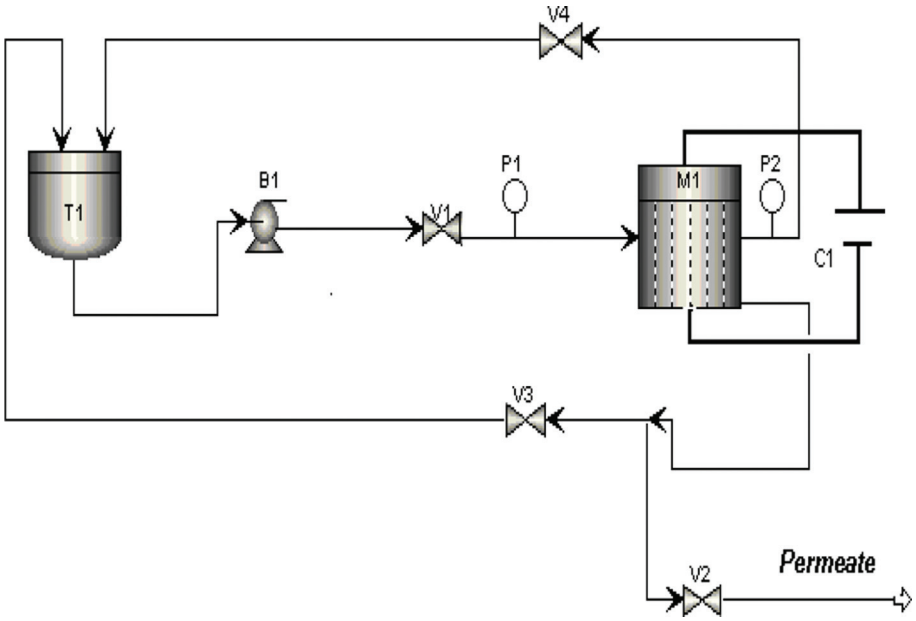

Fig. 2. Schematic representation of the experimental membrane module: (T1) feed tank, (B1) bomb (V1, V2, V3, V4) valves (P1, P2) manometers, (M1) UF membrane, (C1) electrodes.

3. Experimental

3.1. Construction and operation of the electro-cross-flow membrane system

The membrane module was constructed of stainless steel and coupled to porous graphite electrodes and a filtration zinc support (*M1*). The inlet pressure to the membrane module was set by the valve (*V1*) placed between the pump (*B1*) and the pressure gauge (*P1*). The transmembrane pressure was regulated with a valve (*V4*), placed on the side of the rejection stream of the cell, and measured with gauge (*P2*) placed between the cell and the valve. Two valves (*V2*, *V3*) control the recycling of permeate to the feed tank and its collection. The electrodes (*C1*) were connected to a 10 A power supply. The complete set-up is shown in Fig. 2.

The prepared salt solution was pumped through the membrane with a transmembrane pressure of 2.8 bar, permeate and rejected solution were recirculated until the permeate acquired a steady concentration. Then, permeate was collected until recovery of 95% of water. The solution in the tank was maintained at a constant temperature of 25°C. Simultaneously, D.C. voltage was applied and regulated by a power supply and maintained constant from the beginning until the end of each experiment. After each filtration experiment, the membrane was removed, rinsed with deionized water, and stored in refrigeration for later use. The filtration system was washed with 0.02 M HCl solution for 15 min and then rinsing with deionized water until the pH 7. In this work, two kinds of polymeric membranes were used, and prepared according to recent published studies [27,28]. Membrane characteristics such as chemical composition and molecular structure of the two UF membranes used in this study, identified the membranes as without or neutral surface charge (SP1) and negative surface charge (AC1). The main features of the membranes used are shown in Table 1.

3.2. Electro-cross-flow operation system and data acquisition

This study focuses on comparing the performance of an UF membrane system with and without coupled

Table 1
Characteristics of the ultrafiltration membranes used: without surface charge (SP1) and with negative surface charge (AC1)

	Membrane thickness (μm)	Flux (L/m^2 s)	A-Value (kg/Pam^2 s)	Water content (%-wt)	NMWCO (kDa)	Charge density (meq/L m^2)
SP1	127	0.0293	483×10^{-9}	80.2	70–162	–
AC1	165.1	0.0271	120.5×10^{-9}	45.3	70–162	75.5637

electrodes, to evaluate the degree of improvement in the removal of divalent metal ions, found at a concentration that is typical for industrial wastewater. The concentration of metal ions was set at 50 mg/L. We present here the results summary from a series of experiments, in which several membrane structural parameters, and different functional and operational conditions of the filtration system, were tested. Our chief aim was to establish the most effective conditions to maximize metal ion rejection, proper electrode charge and minimize membrane fouling. The experiments were conducted with two types of UF membranes (SP1 and AC1); the membranes were coupled to electrodes in a module with a capacitor that allows operation at fixed voltages of 0.5, 0.75, 1.0, and 1.5 V. Aqueous solutions from three salts ($PbSO_4$, $CaSO_4$ and $FeSO_4$) were prepared at a concentration of 50 ppm. Each salt solution was adjusted to a final pH of 4, 7 and 11. Each experimental module operated at a constant pressure and temperature of 4.8 bar and 25°C, respectively. Experiments were conducted without applying charge on the electrodes, or applying a constant charge of 0.5, 0.75, 1.0, and 1.5 V. Forty-five experiments were performed on each membrane. In every experiment, at 5-minute intervals (from 5 min up to 90 min), the removal of metals was calculated with the following equation:

$$R = \left(1 - \frac{C_P}{C_f}\right). \tag{7}$$

The concentration of heavy metal ions in every solution was determined by atomic absorption spectrometry at their respective wavelength.

4. Application of a neural network

4.1. Deduction of the model

Operation of the back propagation network (BPN) entails learning a set of predefined input–output data pairs given as examples or data for training or learning. In this study, the input data used are time (t) and voltage (v), and the corresponding output value is the mole fraction of ion removal (R). The electromembrane model system resulted in a nonlinear function f, described by the following relationship: $R(t,v) = f(t,v)$.

Several identification experiments were performed by changing the number of neurons of the hidden layers, and using the following sigmoid function to describe node activation:

$$f_k(\mathrm{net}_{jk}) = \frac{1}{1 + e^{-\mathrm{net}_{ij}}}. \tag{5}$$

The general identification algorithm used is described below:

1. Calculation of an input vector (using input/output operational data).
2. Normalization of network input data and rearrangement of data in column vectors.
3. Initialization of the network. Using the initial values of the weights matrices, polarizations, number of hidden layers, number of nodes and the activation function.
4. Training of the neural network using the BPN.
5. Validation of the network. Comparison of the neural network outputs with the real or experimental outputs.

The BPN algorithm was used to adjust the parameters of the multilayer network, with software support for neural networks from the MATLAB (V. 7.0) Toolbox package.

The following code trains the network backpropagation of two inputs, 2 neurons in the hidden layer, and one output with the training algorithm ***trainlm:***

```
net=newff(minmax(a0),[N1 N2],{'logsig' 'purelin'},
'trainlm);
net.trainParam.epochs=500; [net,tr]=train(et,a0,T);
```

Figs. 3 and 4 display the mean square error (mse) in the training phase, comparing when the network runs with one or two neurons in the hidden layers, and only one neuron in the output layer. The analysis was performed using the membrane with negative surface charge, for the removal of Pb^{2+} ions at pH 4.

4.2. Generating the BPN model.

The BPN model was generated with a three layer ANN. Fig. 5 shows the network's architecture, its equations, and components [29,30].

$$a_1^1 = \frac{1}{1 + e^{-\mathrm{net}_1^1}}, \tag{6}$$

$$a_2^1 = \frac{1}{1 + e^{-\mathrm{net}_{21}^1}}. \tag{7}$$

$$a_1^1 = \mathrm{net}_1^2. \tag{8}$$

By replacing the previous equations, the model can be written as follows:

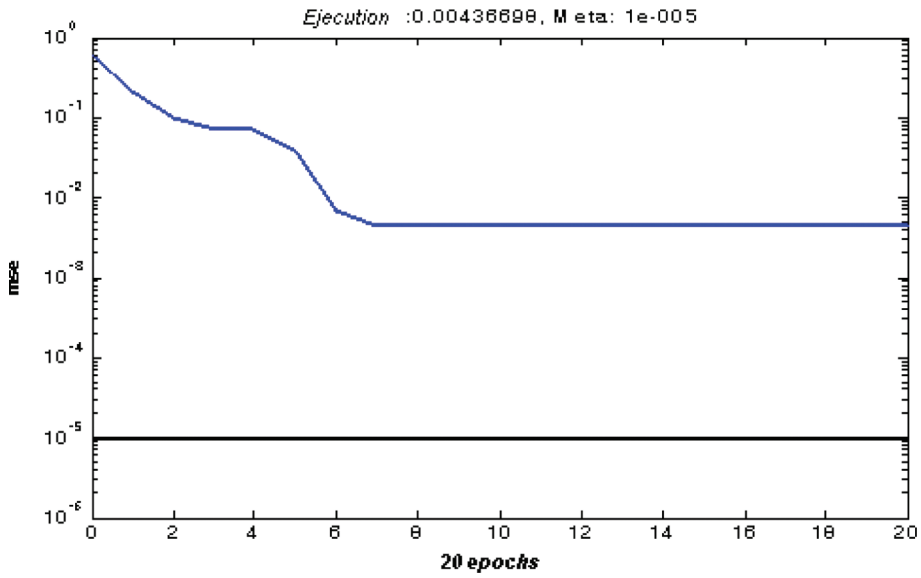

Fig. 3. Training RN; phase 2-1-1.

$$R = a_1^2 = w_{11}^{21}\left(\frac{1}{1+e^{-net_1^1}}\right) + w_{12}^{21}\left(\frac{1}{1+e^{-net_{21}^1}}\right) + b_1^2 \quad (9)$$

where R or a_1^2 is the molar fraction of rejection for a specific ion; the net_i^j of the model is defined by the following equations:

$$net_1^1 = w_{11}^{10}.t + w_{12}^{10}.v + b_1^1 \quad (10)$$

$$net_2^1 = w_{21}^{10}.t + w_{22}^{10}.v + b_2^1 \quad (11)$$

$$net_1^2 = w_{11}^{21}.a_1^1 + w_{12}^{21}.a_1^1 + b_2^1 \quad (12)$$

where t is time in minutes, v voltage in volts, w_i^j the synaptic weight, and b_i^j the bias of the ANN model.

mse was used as an objective function to yield the trained weights and correlation coefficient r were used

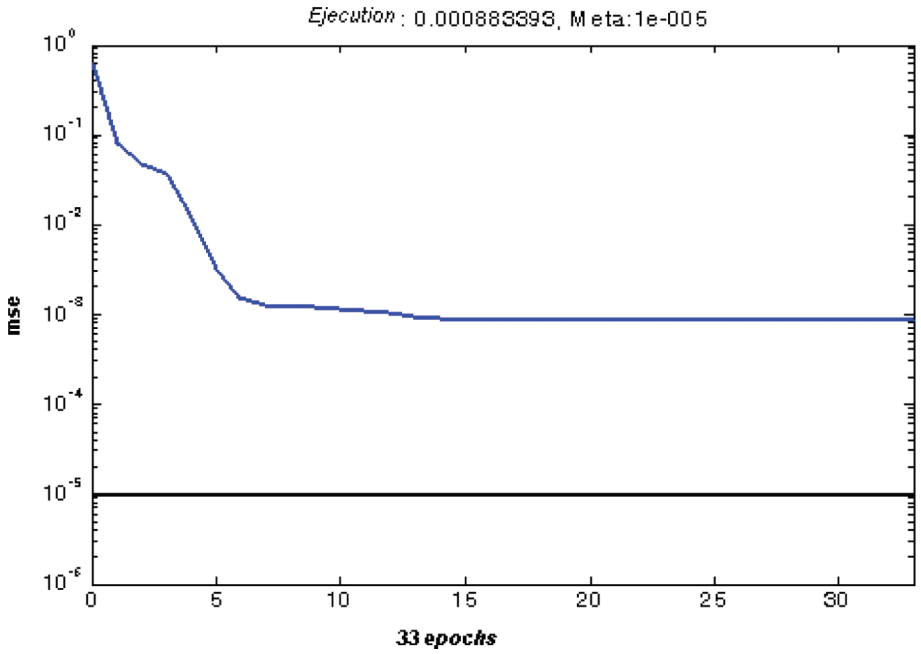

Fig. 4. Training RN; phase 2-2-1.

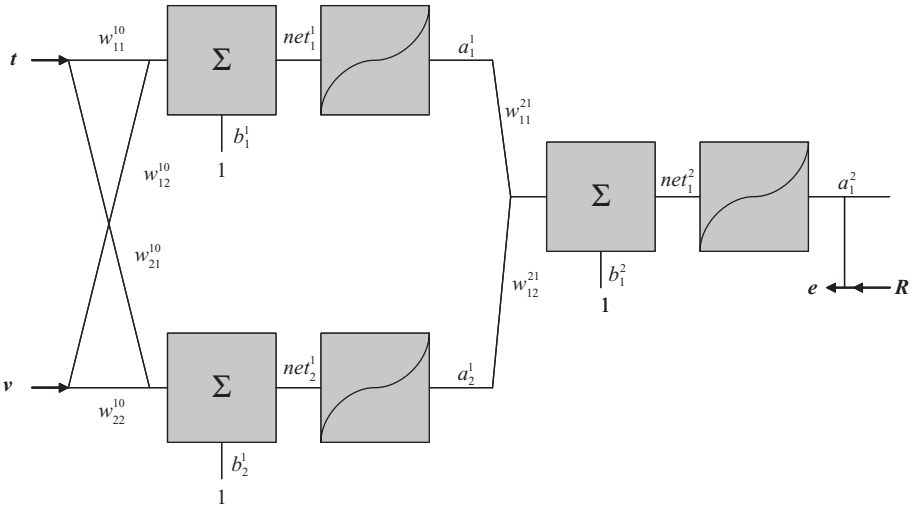

Fig. 5. Architecture of an artificial neuronal network with three layers: entry layer, a hidden layer of two neurons and an exit layer of one neuron.

to qualify the generalization capability of the training network. The expressions to evaluate mse, r^2 and r are evaluated as follows:

$$\text{mse} = \sum_{i=1}^{N} \frac{\left(R_{\text{Exp}} - R_{\text{Model}}\right)^2}{N} \tag{13}$$

$$r^2 = 1 - \frac{\dfrac{\sum_{i=1}^{N}\left(R_{\text{Exp}} - R_{\text{CMode}}\right)^2}{N-q-1}}{\dfrac{\sum_{i=1}^{N}\left(R_E - \bar{R}_{\text{Exp}}\right)^2}{N-1}} \tag{14}$$

$$r = \text{sqrt}\left(r^2\right) \tag{15}$$

To obtain the model ANN was used 90 experimental points, were used 80% for training, and 10% testing and 10% validation.

For analysis of the variables, the model can be simplified to a minimal architecture of three layers with a single neuron (Eq. (9)) where the input is the time and the output the percentage of removal, with the rest of the variables becoming constant. This simplifies the model to a non-linear model with two parameters (b and k):

$$\frac{R_\infty - R}{R_\infty - R_1} = \frac{e^{kt1} + b}{e^{kt} + b} \tag{16}$$

5. Results and discussion

Tables 2–7 show the values of the model parameters obtained from the 18 studied membrane systems, as well as the model's goodness of *fit* $\left(r^2\right)$.

Tables 8–13 show the values of parameters k and b from the simplified ANN model (Eq. (16)) for each of the 18 different conditions at a fixed-voltage.

The system's parameter k showed an 11-fold-increase from zero to 1.5 V.

We generated an equation for each of the 18 models in terms of voltage and the time to calculate the rate of removal. Selection of the appropriate model depended on the type of ion removed (Pb^{2+}, Ca^{2+}, and Fe^{2+}), pH conditions (4, 7 and 11) and the structural features of the membranes (SP1 or AC1). The models obtained are valid only for the conditions of P, T and composition under which the systems were tested. For all models, the goodness of fit was greater than 0.89, which means a confidence interval greater than 89% in predicting the clearance rate compared with experimental values.

Next, we compared the experimental R-value, with the R-value obtained from the neural networks, for a system with an AC1 membrane used for the removal of Pb^{2^*} at pH 4. Figs. 6–10 show the dispersion of the theoretical and experimental values at each voltage, the theoretical R-value percentage as referred to the model can be predicted with a goodness of fit of 0.96. Figs. 6–10 show that the model maintains an increased margin of error when the system is still far away from the R-value percentage required to achieve the stable state. In relation to the previous observation, one can consider that the model fails to adapt the early data collected at the initialization

Table 2
Neuronal model parameters, for systems using a neutral ultra-filtration membrane (SP1), with Pb^{2+}, Ca^{2+}, Fe^{2+} solutions at pH 4

	w_{11}^{10}	w_{12}^{10}	b_1^1	w_{21}^{10}	w_{22}^{10}	b_2^1	w_{11}^{21}	w_{12}^{21}	b_1^2	r^2
Pb^{2+}	0.171	−0.266	−0.174	0.021	5.352	−3.109	0.761	0.926	−0.660	0.964
Ca^{2+}	−0.133	0.160	1.261	0.049	8.509	−5.511	−0.594	0.687	0.297	0.954
Fe^{2+}	0.049	5.821	−6.500	−0.049	−5.783	6.458	−101.7	−102.5	102.7	0.899

Table 3
Neuronal model parameters, for systems using a neutral ultra-filtration membrane (SP1), with Pb^{2+}, Ca^{2+}, Fe^{2+} solutions at pH 7

	w_{11}^{10}	w_{12}^{10}	b_1^1	w_{11}^{10}	w_{22}^{10}	b_2^1	w_{11}^{21}	w_{12}^{21}	b_1^2	r^2
Pb^{2+}	−0.041	4.411	2.147	0.055	2.248	−2.785	0.989	0.895	−0.831	0.954
Ca^{2+}	−0.167	2.810	0.498	0.021	4.431	−2.703	−0.325	1.093	−0.045	0.942
Fe^{2+}	−0.096	0.330	0.262	−0.069	−9.415	7.291	−0.879	−0.654	1.002	0.963

Table 4
Neuronal model parameters, for systems using a neutral ultra-filtration membrane (SP1), with Pb^{2+}, Ca^{2+}, Fe^{2+} solutions at pH 11

	w_{11}^{10}	w_{12}^{10}	b_1^1	w_{11}^{10}	w_{22}^{10}	b_2^1	w_{11}^{21}	w_{11}^{21}	b_1^2	r^2
Pb^{2+}	−0.107	1.993	0.022	0.008	3.985	−1.814	−0.586	1.113	−0.061	0.972
Ca^{2+}	0.021	4.576	−2.925	0.131	−2.529	0.424	0.960	0.623	−0.572	0.981
Fe^{2+}	0.148	−1.136	−0.705	0.022	5.438	−3.107	0.485	0.920	−0.386	0.973

Table 5
Neuronal model parameters, for systems using a charged ultra-filtration membrane (AC1), with Pb^{2+}, Ca^{2+}, Fe^{2+} solutions at pH 4

	w_{11}^{10}	w_{12}^{10}	b_1^1	w_{11}^{10}	w_{22}^{10}	b_2^1	w_{11}^{21}	w_{11}^{21}	b_1^2	r^2
Pb^{2+}	0.084	2.610	−2.775	−0.036	7.568	0.411	0.634	0.784	−0.405	0.990
Ca^{2+}	−0.180	−1.890	5.595	0.008	8.762	−3.453	−0.298	0.783	0.212	0.979
Fe^{2+}	−0.111	0.481	0.683	0.025	5.805	−3.231	−0.415	0.854	0.166	0.979

Table 6
Neuronal model parameters, for systems using a charged ultra-filtration membrane (AC1), with Pb^{2+}, Ca^{2+}, Fe^{2+} solutions at pH 7

	w_{11}^{10}	w_{12}^{10}	b_1^1	w_{11}^{10}	w_{22}^{10}	b_2^1	w_{11}^{21}	w_{11}^{21}	b_1^2	r^2
Pb^{2+}	−0.134	1.246	0.509	0.009	4.513	−1.803	−0.526	0.941	0.090	0.979
Ca^{2+}	−0.076	−0.878	1.883	−0.043	7.158	0.910	−0.826	0.880	0.150	0.986
Fe^{2+}	0.265	0.762	−4.695	0.047	14.131	−6.715	0.255	0.747	−0.009	0.990

Table 7
Neuronal model parameters, for systems using a charged ultra-filtration membrane (AC1), with Pb^{2+}, Ca^{2+}, Fe^{2+} solutions at pH 11

	w_{11}^{10}	w_{12}^{10}	b_1^1	w_{11}^{10}	w_{22}^{10}	b_2^1	w_{11}^{21}	w_{11}^{21}	b_1^2	r^2
Pb^{2+}	0.005	4.040	−1.493	−0.111	1.321	1.221	0.788	−0.500	0.199	0.984
Ca^{2+}	0.024	5.273	−3.422	−0.101	1.716	−0.410	0.793	−0.675	0.212	0.984
Fe^{2+}	−0.119	1.448	0.4071	0.024	5.800	−3.041	−0.513	0.875	0.134	0.977

Table 8
Neuronal model parameters, for systems using a neutral ultra-filtration membrane (SP1), with a Pb^{2+} solution at pH 4, 7 and 11, and fixed-voltages of 0, 0.5, 0.75, 1 and 1.5 V

Pb^{2+}	pH 4			pH 7			pH 11		
V (volts)	*B*	*k* (min^{-1})	r^2	*b*	*k* (min^{-1})	r^2	*b*	*k* (min^{-1})	r^2
0	19.2885	0.0745	0.9926	2.4923	0.0578	0.9252	1.0645	0.0503	0.9660
0.5	3.4339	0.1498	0.9958	2.8322	0.1088	0.9670	7.9322	0.1206	0.9970
0.75	11.2498	0.1379	0.9926	22.7412	0.0858	0.9912	4.4014	0.0755	0.9958
1	3.579	0.1867	0.9976	6.1579	0.1822	0.9994	5.8187	0.0783	0.9924
1.5	−1.2495	0.1196	0.9942	58.6113	0.3346	0.9966	12.4511	0.132	0.9916

Table 9
Neuronal model parameters, for systems using a neutral ultra-filtration membrane (SP1), with a Ca^{2+} solution at pH 4, 7 and 11, and fixed-voltages of 0, 0.5, 0.75, 1 and 1.5 V

Ca^{2+}	pH 4			pH 7			pH 11		
V (volts)	*B*	*k* (min^{-1})	r^2	*b*	*k* (min^{-1})	r^2	*b*	*k* (min^{-1})	r^2
0	1.372	0.055	0.9751	2.1372	0.0415	0.9187	5.7678	0.0585	0.9789
0.5	2.929	0.089	0.9988	2.8619	0.0898	0.9882	2.1705	0.066	0.9908
0.75	5.861	0.1173	0.9960	3.629	0.0648	0.9850	18.2948	0.1294	0.9916
1	−0.272	0.0528	0.9978	52.0929	0.1568	0.9922	8.1597	0.1343	0.9853
1.5	1.347	0.1439	0.9920	23.1384	0.2302	0.9906	14.0857	0.1198	0.9974

Table 10
Neuronal model parameters, for systems using a neutral ultra-filtration membrane (SP1), with a Fe^{2+} solution at pH 4, 7 and 11, and fixed-voltages of 0, 0.5, 0.75, 1 and 1.5 V

Fe^{2+}	pH 4			pH 7			pH 11		
V (volts)	*B*	*k* (min^{-1})	r^2	*b*	*k* (min^{-1})	r^2	*b*	*k* (min^{-1})	r^2
0	3.1218	0.0707	0.9822	6.262	0.0918	0.9761	15.33	0.0768	0.9846
0.5	12.7232	0.0939	0.9828	12.7232	0.0939	0.9940	12.6174	0.1352	0.9888
0.75	3.4533	0.1002	0.9940	3.4533	0.1002	0.9988	9.387	0.1284	0.9868
1	5.0052	0.1074	0.9954	5.0052	0.1074	0.9976	3.8927	0.1232	0.9962
1.5	1.9547	0.1548	0.9904	1.9547	0.1548	0.9896	8.4751	0.1885	0.9968

Table 11
Neuronal model parameters for systems using a charged ultra-filtration membrane (AC1), with a Pb^{2+} solution at pH 4, 7 and 11, and fixed-voltages of 0, 0.5, 0.75, 1 and 1.5 V

Pb^{2+}	pH 4			pH 7			pH 11		
V (volts)	*B*	*k* (min^{-1})	r^2	*b*	*k* (min^{-1})	r^2	*b*	*k* (min^{-1})	r^2
0	11.1527	0.0654	0.9862	9.9395	0.0907	0.9936	5.3575	0.0953	0.9813
0.5	28.816	0.2406	0.9940	7.7335	0.1233	0.9922	7.6874	0.1071	0.9870
0.75	16.8781	0.1684	0.9922	14.5182	0.1341	0.9972	3.7715	0.0906	0.9920
1	3.579	0.1867	0.9976	36.3592	0.2226	0.9980	9.4692	0.1001	0.9936
1.5	12.3843	0.339	0.9994	16.9296	0.2	0.9978	18.0968	0.1143	0.9902

Table 12
Neuronal model parameters, for systems using a charged ultra-filtration membrane (AC1), with Ca^{2+} solution at pH 4, 7 and 11, and fixed-voltages of 0, 0.5, 0.75, 1 and 1.5 V

Ca^{2+}	pH 4			pH 7			pH 11		
V (volts)	B	k (min^{-1})	r^2	b	k (min^{-1})	r^2	b	k (min^{-1})	r^2
0	29.276	0.0854	0.9910	1.5865	0.0579	0.9908	1.4559	0.0512	0.9688
0.5	11.5865	0.1343	0.9962	4.2911	0.128	0.9894	15.0723	0.0955	0.9934
0.75	42.9275	0.1501	0.9968	5.7032	0.1035	0.9906	4.1874	0.0862	0.9944
1	7.0207	0.1412	0.9978	3.2626	0.0954	0.9655	15.4127	0.1364	0.9926
1.5	6.2921	0.1732	0.9948	14.2139	0.1516	0.9896	6.4911	0.1085	0.9930

Table 13
Neuronal model parameters, for systems using a charged ultra-filtration membrane (AC1), with a Fe^{2+} solution at pH 4, 7 and 11, and fixed-voltages of 0, 0.5, 0.75, 1 and 1.5 V

Fe^{2+}	pH 4			pH 7			pH 11		
V (volts)	B	k (min^{-1})	r^2	b	k (min^{-1})	r^2	b	k (min^{-1})	r^2
0	5.9908	0.0523	0.9822	1.0181	0.035	0.9775	7.7254	0.0528	0.9860
0.5	12.2897	0.1107	0.9828	18.7095	0.1758	0.9962	14.0146	0.0992	0.9962
0.75	13.0817	0.1184	0.9940	11.8694	0.1841	0.9962	7.2266	0.1171	0.9906
1	6.2153	0.1271	0.9954	23.1389	0.2302	0.9606	16.7745	0.1404	0.9972
1.5	3.0149	0.1835	0.9904	68.3656	0.3888	0.9990	12.1762	0.1446	0.9902

of the system. This may suggest the need to perform experimental measurements at smaller time intervals (less than five minutes) so that the model can adequately predict and explain the rate of ion rejection under the established conditions.

We were able to establish the conditions at which the maximum rejection value is achieved, in the studied models, and thus predict the capacity of the system. An analysis of the model's behavior was performed, under the following conditions: time, from zero to infinite, and voltage from zero to 1.5 V. The results are summarized in Figs. 11 and 12. They show simultaneously the behavior of variables such as time (t), voltage (V) and percentage of removal ($\%R$) using two types of membranes: SP1 and AC1. In these systems the maximum rejection value (99%) is reached when t is equal or higher than 30 min, and V is greater than 0.75 V. Figs. 11 and 12 also shows, that the AC1 membrane has a higher rate of removal than the SP1 membrane, but

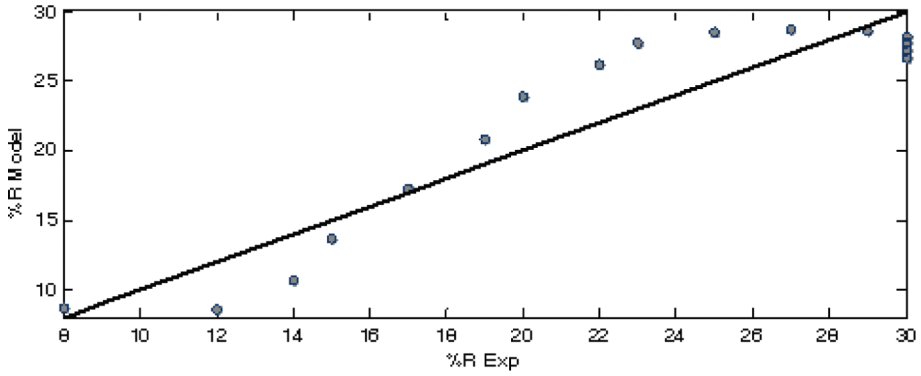

Fig. 6. Comparison between the experimental removal percentage ($\%R$) and the R-value obtained by the model. The data was collected from a system with a negative charge membrane (AC1) for the removal Pb^{2+} ions at pH 4 and 0 volts.

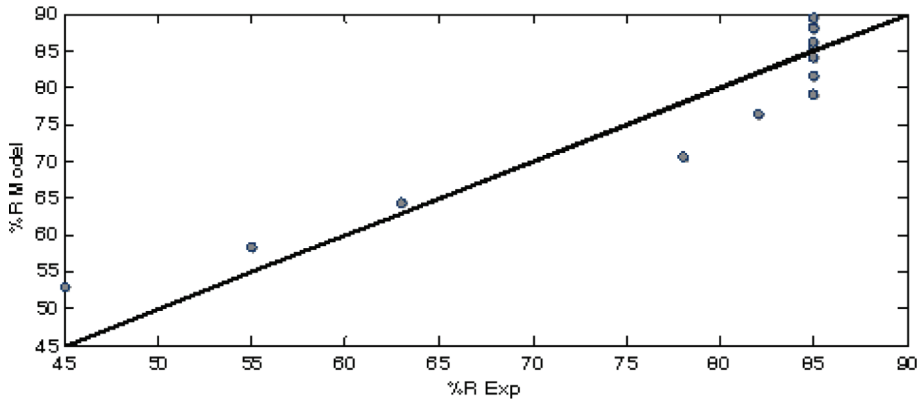

Fig. 7. Comparison between the experimental removal percentage (%*R*) and the *R*-value obtained by the model. The data was collected from a system with a negative charge membrane (AC1) for the removal Pb^{2+} ions at pH 4 and 0.5 V.

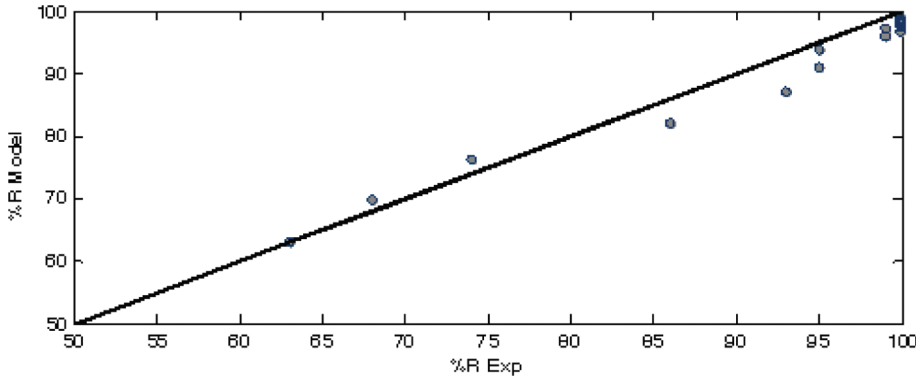

Fig. 8. Comparison between the experimental removal percentage (%*R*) and the *R*-value obtained by the model. The data was collected from a system with a negative charge membrane (AC1) for the removal Pb^{2+} ions at pH 4 and 0 volts and 0.75 V.

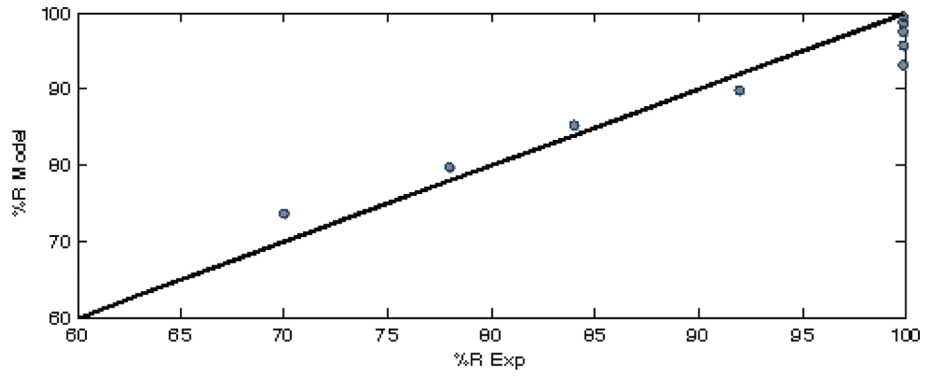

Fig. 9. Comparison between the experimental removal percentage (%*R*) and the *R*-value obtained by the model. The data was collected from a system with a negative charge membrane (AC1) for the removal Pb^{2+} ions at pH 4 and 1.0 V.

eventually both are able to reach the same percentage of removal (>99%).

6. Conclusions

Membrane technology applications have been evolving rapidly as manufacturers have developed improvements to the physical and chemical properties of membranes, as wells as the engineering processes related to them. In this work, our studies focused on membrane technologies used for the removal of common pollutants found in industrial wastewater, and in particular those that operate with processes driven by pressure difference. These processes are based on

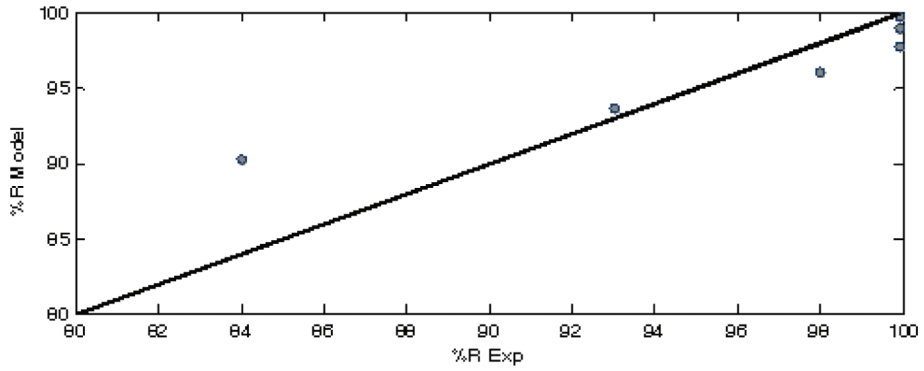

Fig. 10. Comparison between the experimental removal percentage (%*R*) and the *R*-value obtained by the model. The data was collected from a system with a negative charge membrane (AC1) for the removal Pb^{2+} ions at pH 4 and 1.5 V.

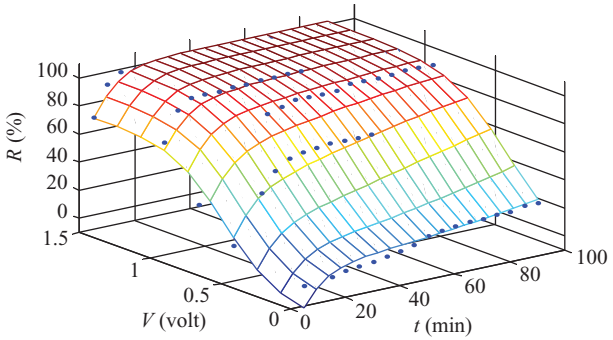

Fig. 11. Comparison between the experimental data and the model's predictions ($r^2 = 0.964$), for the system using the SP1 membrane for removal of Pb^{2+} ions at pH 4 and voltages from 0 to 1.5 V.

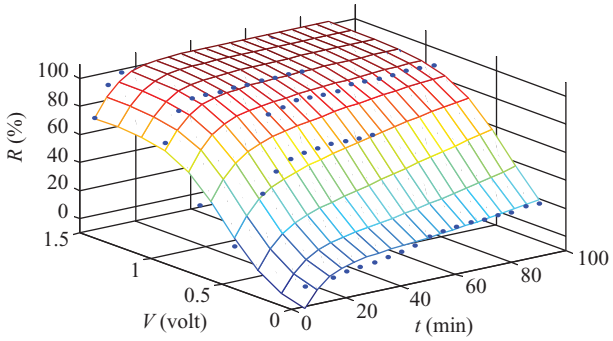

Fig. 12. Comparison between the experimental data and the model's predictions ($r^2 = 0.99$), for the system using the AC1 membrane for removal of Pb^{2+} ions at pH 4 and voltages from 0 to 1.5 V.

the use of selective permeable membranes; their efficiency is dependent on the size and distribution of its pores and in some cases on the use of electrical potential. Our objective was the development of an UF membrane system coupled to electrodes, which would be effective for the removal of metal ions at concentrations typically found in wastewater. We intended to assess whether the electrical field acts as a force, which in addition to the selectivity of the membrane promotes the removal of substances in ionic form. To incorporate electrical field forces into the system we developed an electro-cross-flow module, and selected membranes designed for UF. We provided conditions for the system to be effective for filtration of wastewater containing concentrations of heavy metals in ionic form. To maintain adequate permeate flow, the system's pressure was set low, lower than that required for NF or RO membranes having the same working flow. Membrane technologies are evaluated based on solute selectivity; permeate production and/or flow and the membrane's useful half-life. The electrodes allow the system to maintain an adequate working flow without resorting to higher pressures. Working at lower pressures avoids clogging the membrane pores, given that fewer ions will try to cross the membrane, as they are attracted to the electrode. This also prevents the formation of a polarization layer on the surface as ions are kept away from it. Although the mechanism described above suggests a way, in which the membranes should function. The system was not evaluated in regards to a decrease in flow or pressure. The effectiveness of the system was assessed in terms of its selectivity and/or capacity for the removal of divalent ions by determining their concentration in the permeate. Functional and design characteristics of the system were chosen to incorporate favorable conditions of operation and to set the values of variables such as time and voltage in order to reach the maximum rate of rejection (> 99%) for all ions simultaneously. Our results show that ion removal higher than 99% can be accomplished by using voltages lower than 1.5 V. Applying voltage to the system improves ion removal by over 60%. The removal percentages

obtained in all of our experiments suggest that pH does not have a significant effect in the separation process. We used diluted ion solutions (50 mg/L) in our experiments to ensure complete dissociation of the ionic species present. Hence, although pH does not affect the final percentage, it does however, slow the removal process in the first 30 min. Further analysis of the experimental data does not show that membrane surface charge affects the overall removal process. However, the neutral membrane (SP1) generates a higher flux (0.293 L/m^2 s), than the charged membrane (AC1) (0.271 L/m^2 s). This does affect the amount of water recovered from the process, but not the total removal of ions. Our experimental data also show that all the ions studied are efficiently removed by applying voltage. In every case, applying a voltage of 1.0 V for a period of 30 min to an AC1 membrane, the system removes over 90% of the ions present. The ANN model developed, allowed us to properly adjust the experimental data through a nonlinear model and predict with a deviation no greater than 10% the removal rate as a function of voltage and time. In addition, a simplified version of the previous model allowed us to predict the removal percentage as a function of time only at a fixed voltage. Finally, it permitted us to observe the speed with which the system stabilized to achieve the maximum removal percentage.

Symbol

a_1^2	molar fraction of rejection for a specific ion
b_i^j	the bias
b	a dimensional parameter
C_f	concentrations in feed
C_p	concentrations in permeated
f	nonlinear function
k	rate parameter (min^{-1})
R_{Exp}	experimental percentage remotion
R_{Model}	predicted value of percentage remotion
$\bar{R}_{Exp}$	mean of experimental percentage remotion
q	number of parameters consider in the ANN model
N	number of data points
R	molar fraction of rejection for a specific ion
R_1	molar fraction of rejection for a specific ion at t_1
R_∞	molar fraction of rejection for a specific ion at t_∞
r^2	goodness of fit model
t	time elapsed since the time t_1 (min)
t_1	elapsed time since the system boot time (min)
v	voltage (V)
w_i^j	the synaptic weight

References

[1] W.R. Bowen, M.G. Jones, J.S. Webfoot and H.N.S Yousef, Predicting salt rejections at nanofiltration membranes using artificial neural networks, Desalination, 129 (2000) 147–162.

[2] N. Hilal, M. Al-Abri, H. Al-Hinai and M. Abu-Arabi. Characterization and retention of NF membranes using PEG, HS and polyelectrolytes, Desalination, 221 (2008) 284–293.

[3] A.R. Hassan, N.A. Ali, N. Abdull and A.F. Ismail, A theoretical approach on membrane characterization: the deduction of fine structural details of asymmetric nanofiltration membranes, Desalination, 206 (2007) 107–126.

[4] T. Tsuru, M. Urairi, S.I Nakao and S. Kimura, Reverse osmosis of single and mixed electrolytes with charged membranes: experiment and analysis, J. Chem Eng. Jpn., 24 (1991) 518–524.

[5] S. Pérez-Sicairos, S.W. Lin, R.M. Félix-Navarro and H. Espinoza-Gómez, Rejection of As(III) and As(V) from arsenic contaminated water via electro-cross-flow negatively charged nanofiltration membrane system, Desalination, 249 (2009) 458–465.

[6] T. Akiki, W. Charon, M.C. Iltchev, G. Accary and R. Kouta, Influence of local porosity and local permeability on the performances of a polymer electrolyte membrane fuel cell, J. Power Sour., 195 (2010) 5258–5268.

[7] W. Zhang, J. Li, G. Chen, W. You and Z. Ren. Simulations of solute concentration profile and mass transfer behavior near the membrane surface with finite volume method, J. Membr. Sci., 355 (2010) 18–27.

[8] M. Sadrzadeh, T. Mohammadi, J. Ivakpur and N. Kasiri, Separation of lead ions from wastewater using electrodialysis: Comparing mathematical and neural network modeling, Chem. Eng. J., 144 (2008) 431–441.

[9] H. Espinoza-Gómez, S.W. Lin and E. Rogel-Hernández, Development of energy-saving spinning membrana system and negatively charged ultrafiltation membranes for recovering oil from waste machine cutting fluid, Heat Mass Transf., 41 (2005) 503–209.

[10] J. Schaep, B. Van der Bruggen, C. Vandecasteele and D. Wilms, Influence of ion size and charge in nanofiltration, Sep. Purif. Technol., 14 (1998) 155–162.

[11] G. Cybenko, Approximation by superpositions of a sigmoidal function, Math Control Signal, 2 (1989) 303–314.

[12] J. Misra and I. Saha, Artificial Neural Network in hardware: A survey of two decades of progress, Neurocomputing, 74 (2010) 239–255.

[13] M. Dornier, M. Decloux, G. Trystram and A. Lebert, Dynamic modeling of crossflow microfiltration using neural networks, J. Membr. Sci., 98 (1995) 263–273.

[14] M. Hamachi, M. Cabassud, A. Davin and M.M. Peuchot, Dynamic modelling of crossflow microfiltration of bentonite suspension using recurrent neural networks, Chem. Eng. Process., 38 (1999) 203–210.

[15] W.R. Bowen, M.G. Jones and H.N. Yousef, Dynamic ultrafiltration of proteins – A neural network approach, J. Membr. Sci., 146 (1998) 225–235.

[16] C. Teodosiu, O. Pastravanu and M. Macoceanu, Neural network models for ultrafiltration and backwashing, Wat. Res., 34 (2000) 4371–4380.

[17] N. Delgrange, C. Cabassud, M. Cabassud, L. Duran-Bourlie and J.M. Laine, Neural networks for prediction of ultrafiltration transmembrane pressure – application to drinking water production, J. Membr. Sci., 150 (1998) 111–123.

[18] H.R. Godini, M. Ghadrdan, M.R. Omidkhah and S.S. Madaeni, Part II: Prediction of the dialysis process performance using Artificial Neural Network (ANN), Desalination, 265 (2011) 11–21.

[19] B.K. Nandi, A. Moparthi, R. Uppaluri and M.K. Purkait, Treatment of oily wastewater using low cost ceramic membrane:

Comperative assessment of pore blocking and artificial neural network models, Chem. Eng. Res. Des., 88 (2010) 881–892.
[20] S.S. Madaeni, N.T. Hasankiadeh, A.R. Kurdian and A. Rahimpour, Modeling and optimization of membrane fabrication using artificial neural network and genetic algorithm, Sep. Purif. Technol., 76 (2010) 33–43.
[21] Q.F. Liu, S.H. Kim and S. Lee, Prediction of microfiltratiom membrane fouling using artificial neural network models, Sep. Purif. Technol., 70 (2009) 96–102.
[22] M. Sadrzadeh, T. Mohammadi, J. Ivakpour and N. Kasiri, Neural Network modeling of Pb^{2+} removal from wastewater using electrodialysis, Chem. Eng. Process., 48 (2009) 1371–1381.
[23] W.R. Bowen, M.G. Jones and H.N.S. Yousef, Prediction of the rate of crossflow membrane ultrafiltration of colloids: A neural network approach, Chem. Eng. Sci., 53 (1998) 3793–3802.
[24] H. Chen and A.S. Kim, Prediction of permeate flux decline in crossflow membrane filtration of colloidal suspension: a radial basis function neural network approach, Desalination, 192 (2006) 415–428.
[25] K.J. Hunt, D. Sbarbaro, R. Zbikowski and P.J. Gawthrop, Neural networks for control systems—A survey, Automatica, 28 (1992) 1083–1112.
[26] V.D. Nguyen, R.R. Tan, Y. Brondial and T. Fuchino, Prediction of vapor–liquid equilibrium data for ternary systems using artificial neural networks, Fluid Phase Equilibr., 254 (2007) 188–197.
[27] H. Espinoza Gómez and S.W. Lin, Development of Acrylonitrile co-polymers Ultrafiltration Membranes, Polymer Bull., 3 (2001) 297–304.
[28] H. Espinoza Gómez and S.W. Lin, Development of hydrophilic ultrafiltration membrane from polisulfone-polivinylpyrrolidone, Rev. Soc. Quím. Méx., 47 (2003) 53–57.
[29] M.T. Hagan, H.B. Demuth and M.H. Beale, Neural Network Design, Boston, MA: PWS Publishing 1996.
[30] D.E. Rumelhart, G.E. Hinton and R.J. Williams, Learning representations by back-propagating errors, Nature, 323 (1986) 533–536.